Oligomerization of the Human ABC Transporter ABCG2: Evaluation of the Native Protein and Chimeric Dimers†

Aarti Bhatia,‡ Hans-Jochen Schäfer,§ and Christine A. Hrycyna*,‡

Department of Chemistry and Purdue Cancer Center, Purdue University, West Lafayette, Indiana 47907-2084, and Fachbereich Chemie und Pharmazie Institut für Biochemie, Johannes Gutenberg-Universität, Becherweg 30, D-55099 Mainz, Germany

Received February 28, 2005; Revised Manuscript Received June 15, 2005

ABSTRACT: Human ABCG2, a member of the ATP binding cassette (ABC) transporter superfamily, is overexpressed in numerous multidrug-resistant cells in culture. Localized to the plasma membrane, ABCG2 contains six transmembrane segments and one nucleotide binding domain (NBD) and is thought to function as a dimer or higher order oligomer. Chimeric fusion proteins containing two ABCG2 proteins joined either with or without a flexible linker peptide were expressed at the plasma membrane and maintained drug transport activity. Expression of an ABCG2 variant mutated in a conserved residue in the Walker B motif of the NBD (D210N) resulted in a non-functional protein expressed at the cell surface. Expression of an ABCG2 chimeric dimer containing the D210N mutation in the first ABCG2 resulted in a dominant-negative phenotype, as the protein was expressed at the surface but was not functional. Using a bifunctional photoaffinity nucleotide analogue and a non-membrane-permeable cysteine-specific chemical cross-linking agent, a dimer is the predominant form of oligomerized ABCG2 under our assay conditions. Furthermore, these experiments demonstrated that the dimer interface includes, but may not be limited to, interactions between residues in each monomeric NBD and separate disulfide interactions between the cysteines in the third extracellular loop of each monomer. By changing all three extracellular cysteines to alanine, we showed that although extracellular disulfide bonds may exist between monomers, they are not essential for ABCG2 localization, transport activity, or prazosin-stimulated ATPase activity. Together, these data suggest that ABCG2 functions as a dimer, but do not exclude functional higher order oligomers.

Human ABCG2, also known as MXR/BCRP/ABCP, is a member of the ATP binding cassette (ABC)[1] transporter family. This 655 amino acid transporter, which is localized to the plasma membrane (*1*), is predicted to have one transmembrane domain (TMD) comprised of six transmembrane segments and one nucleotide binding domain (NBD) (*2*, *3*). ABCG2 is considered a half-transporter and is thought to form a dimer or higher order oligomer (*4*−*6*) because numerous other ABC transporters are roughly twice the molecular weight and have two NBDs and two or more TMDs (*7*−*9*). Originally cloned from cells selected for multidrug resistance (*10*−*12*), endogenous ABCG2 expression has been detected in the placenta, ovary, kidney, breast epithelial cells, small intestine, blood brain barrier, and stem cells (*13*−*18*), with placental expression being distinctly higher than in the other tissues (*14*).

Several eukaryotic half-transporters are known to exist functionally as dimers. The peroxisomal half-transporter ALDP (ABCD1) can homodimerize or heterodimerize with related ABC half-transporters ALDPR (ABCD2) or PMP70 (ABCD3), and interference with dimerization disrupts function (*19*). The half-transporters TAP1 and TAP2, which play a pivotal role in the major histocompatibility complex class I antigen presentation pathway, form a heterodimer that is localized to the endoplasmic reticulum membrane (*20*). The sterol half-transporters ABCG5 and ABCG8 must heterodimerize in order to get to the cell surface (*21*, *22*). Mdl1p, a structural and functional yeast homologue of the TAP transporter, has also been found to exist functionally as a dimer (*23*). Currently, all evidence suggests that ABCG2 homodimerizes but the existence of heterodimers with different half-transporter partners has not been conclusively ruled out (*2*, *3*, *24*−*26*). Recent evidence also suggests that dimerization can occur in intracellular membranes, especially the endoplasmic reticulum (*26*), and glycosylation of ABCG2 does not appear to be essential for dimerization or trafficking to the cell surface (*27*, *28*) (A. Bhatia and C. A. Hrycyna, unpublished data).

Functional biochemical studies of the homologous full-transporter P-glycoprotein (P-gp) and other ABC transporters demonstrated that both of the NBDs are required for substrate transport function (*29*−*34*). Furthermore, structural data have suggested that the catalytic cycle begins with an ATP-induced dimerization of the NBDs (*35*, *36*), further supporting the hypothesis that two NBDs are required for ATP hydrolysis. The current model of NBD dimerization indicates

† This work was supported in part by American Cancer Society Institutional Research Grant IRG-58-006-41 to C.A.H. A.B. is a recipient of the Biochemistry and Molecular Biology Program, NIH Predoctoral Training Grant GM008737.

* Corresponding author. Tel: 765-494-7322. Fax: 765-494-0239. E-mail: hrycyna@purdue.edu.

‡ Purdue University.

§ Johannes Gutenberg-Universität.

[1] Abbreviations: ABC, ATP binding cassette; NBD, nucleotide binding domain; TMD, transmembrane domain; EC, extracellular; β-ME, β-mercaptoethanol; SDS−PAGE, sodium dodecyl sulfate−polyacrylamide gel electrophoresis.

10.1021/bi0503807 CCC: $30.25
Published on Web 07/22/2005

that the Walker A motif from one NBD and the signature sequence from the second NBD interact to form the ATP binding pocket (*35*, *36*). Therefore, it has been hypothesized that ATP binding may also be important for the dimerization of the half-transporter members of the ABC transporter superfamily.

In this study, we characterized the oligomeric state of ABCG2 using various approaches in both drug-selected and transiently transfected cell lines. Chimeric ABCG2 transporters were generated to study ABCG2 as a covalent dimer. We found that these artificial forced dimers were expressed at the plasma membrane by biotinylation and cell surface antibody labeling experiments and were functional for drug transport activity by fluorescent drug accumulation assays. However, when the first gene was rendered non-functional by mutation of the conserved Asp210 residue in the Walker B motif, the dimer was no longer functional. These data together suggest that both ATP sites are essential for activity and that ABCG2 functions as a dimer. Using both photoaffinity and chemical cross-linking techniques, we demonstrated that ABCG2 can form dimers under reducing conditions and that the interface between monomers includes, at a minimum, interactions between the NBDs as well as disulfide linkages between cysteines in the third predicted extracellular loop of each mononer. We also showed that the extracellular disulfide bridges are not essential for function and, thus, are presumably not critical for dimerization.

EXPERIMENTAL PROCEDURES

Materials. Rhodamine 123, doxorubicin (Adriamycin), verapamil, prazosin, mitoxantrone, ATP, sodium orthovanadate, oubain, Tween-20, EGTA, and β-mercaptoethanol (β-ME) were obtained from Sigma-Aldrich (St. Louis, MO). AEBSF, DTT, and aprotinin were purchased from Fisher Scientific (Pittsburgh, PA), and micrococcal nuclease was purchased from Worthington (Lakewood, NJ). Recombinant vaccinia virus (vTF7-3) was a kind gift from Dr. Steven Broyles (Purdue University), and the pTM1 plasmid was a kind gift from Dr. Bernard Moss (NIAID, NIH). HeLa and MCF-7 cells were a generous gift from Dr. Michael Gottesman (NCI, NIH), and MCF-7/AdVp3000 cells were a generous gift from Dr. Susan Bates (NCI, NIH). 8-diN_3-AP_4A was synthesized and provided by Dr. Hans-Jochen Schäfer (Johannes Gutenberg-Universität, Mainz, Germany) (*37*, *38*).

ABCG2 Genotype. Wild-type ABCG2 has an arginine at position 482; however, in drug-selected cell lines this residue has been mutated to either a glycine or threonine, which gives the transporter a wider substrate specificity (*12*, *39*−*42*). All experiments detailed in this paper make use of these gain-of-function mutations, either R482T in the MCF-7/AdVp3000 cell line or R482G in the transiently transfected HeLa cells.

Cell Culture, Transfection, and Crude Membrane Preparation. HeLa cells (cervical epitheliod carcinoma) were cultured in DMEM complete media at 37 °C. ABCG2 (R482G) was overexpressed by transient transfection using the T7 vaccinia virus system as described previously (*43*). ABCG2 monomers, chimeric dimers, D210N variants, and extracellular cysteine-less variants were cloned into the pTM1 vector where expression was under the control of the T7 promoter. The empty vector pTM1 served as the negative control for all transient transfection experiments. MCF-7 cells (breast adenocarcinoma) selected and maintained in 3 μg/mL doxorubicin and 5 μg/mL verapamil (MCF-7/AdVp3000) overexpress ABCG2 (R482T) at the plasma membrane. The negative control for experiments using MCF-7/AdVp3000 cells was the parental cell line MCF-7. To isolate crude membrane fractions, HeLa cells were harvested 48 h post-transfection, and MCF-7/AdVp3000 cells were harvested 48 h post-plating. Crude membrane extracts were prepared as described previously (*43*) with the only exception being that the membrane fraction was pelleted at 300000*g* for 40 min at 4 °C. The membrane pellet was collected, and the membranes were assayed for total protein concentration, aliquoted, frozen on dry ice, and stored at −80 °C until use.

*Cloning and Expression of ABCG2-ABCG2, ABCG2-M-ABCG2, ABCG2-P-ABCG2, ABCG2 (D210N), ABCG2 (D210N)-ABCG2, and ABCG2*Δ*EC-C.* ABCG2-ABCG2, ABCG2-M-ABCG2, and ABCG2-P-ABCG2 were cloned into the pTM1 vector, a mammalian expression plasmid containing a T7 promoter. ABCG2-ABCG2 encodes two identical ABCG2 (R482G) proteins connected by a *Sac*II restriction enzyme site which adds a proline−arginine linker (PR). ABCG2-M-ABCG2 encodes two ABCG2 (R482G) proteins linked by the sequence (PR-NEVELENAADE-SKSEIDALEMSSNDSRSSLIRKRSTRRSVRGSQAQDR-KLSTKEALD-PR) derived from the flexible linker region of human P-glycoprotein. ABCG2-P-ABCG2 encodes two ABCG2 (R482G) proteins linked by the sequence (PR-KRMKKRGVLTEKNANDPENVGERSDLSSDRKMLQ-ESSEEESDTYGEIGLSKSEAIFHWRNLCYEVQIKAE-PR) derived from the flexible linker region of yeast ABC transporter PDR5. The linkers from both MDR1 and PDR5 are flanked by *Sac*II restriction enzyme sites for cloning into the ABCG2-ABCG2 construct. Correct orientation of the linker regions was confirmed by DNA sequencing. ABCG2 (D210N) was constructed by site-directed mutagenesis of aspartate 210 of the parent plasmid pTM1-ABCG2 (R482G). ABCG2 (D210N)-ABCG2 was built using a combination of ABCG2 (D210N) and ABCG2-ABCG2; ABCG2 (D210N) was altered to include a *Sac*II site immediately upstream of the *Xho*I site. The stop codon was then deleted, and the *Sac*II to *Xho*I fragment from ABCG2-ABCG2 (the second gene of the chimeric dimer) was inserted in the pTM1-ABCG2 (D210N) vector. ABCG2ΔEC-C, which contains all three endogenous extracellular cysteines replaced with alanine (C592A, C603A, C608A), was constructed by site-directed mutagenesis of the parent plasmid pTM1-ABCG2 (R482G). All constructs were verified by bidirectional DNA sequencing.

SDS−PAGE and Immunoblot Analysis. Twenty-four hours post-infection/transfection (HeLa) or post-plating (MCF-7/AdVp3000), cells were harvested and lysed in buffer [100 mM Tris, pH 8.0, 0.1% Triton X-100, 10 mM $MgSO_4$, 2 mM $CaCl_2$, 1% (v/v) aprotinin, 2 mM AEBSF, and 50 units/mL micrococcal nuclease] plus either DTT (1 mM) or iodoacetic acid (10 mM). Protein samples were prepared in an appropriate amount of 5× Laemmli-type SDS sample buffer (*44*) with or without β-mercaptoethanol (β-ME) (3.575 M). Protein samples were incubated at room temperature for 30−45 min, and the proteins were separated by SDS−PAGE

(7.5% gels) and transferred to a 0.45 μm nitrocellulose membrane. The membrane was blocked in 20% (w/v) dry nonfat milk dissolved in PBST [phosphate-buffered saline with 0.05% (v/v) Tween-20] at room temperature for 2 h. The membrane was washed and probed with the ABCG2-specific monoclonal antibody BXP-21 (Kamiya Biomedicals, Seattle, WA) at a dilution of 1:1000 in 5% (w/v) nonfat milk in PBST, followed by washing and incubation with an HRP-conjugated goat anti-mouse secondary antibody (1:4000) (Caltag, Burlingame, CA). The immunoprotein complexes were detected using enhanced chemiluminescence (ECL) (Pierce, Rockford, IL).

Cell Surface Biotinylation. For cell surface biotinylation studies, 500000 HeLa cells were plated per well of a six-well plate. Twenty-four hours post-infection/transfection, intact cells were incubated with 500 μL of 1.5 mg/mL nonpermeable biotinylating agent, sulfo-NHS-biotin (Pierce, Rockford, IL), at 4 °C for 1 h with gentle agitation. Cells were washed with buffer containing 100 mM glycine to bind excess biotin prior to cell lysis. Cells were solubilized with RIPA buffer (10 mM Tris, pH 7.4, 150 mM NaCl, 1% Triton X-100, 1% deoxycholate, 0.1% SDS, 1 mM EDTA, 1% aprotinin, 2 mM AEBSF, 1 μg/mL leupeptin, 1 μg/mL pepstatin, 100 μg/mL trypsin inhibitor, and 1 mM iodoacetic acid) for 30 min at 4 °C. Cellular debris was removed by centrifugation at 15800*g* for 30 min at 4 °C, and the supernatant containing the solubilized proteins was incubated with monomeric avidin beads (Pierce, Rockford, IL) at room temperature for 1 h with rotation. Unbound proteins were washed from the beads with RIPA buffer, and the avidin-bound biotinylated proteins were eluted with 1× Laemmli-type SDS protein sample buffer.

Antibody Labeling of Cell Surface Proteins. Determination of cell surface expression by antibody staining was performed as described previously (*43*) with slight modifications. For detection of cell surface ABCG2, 500000 cells were labeled with the anti-ABCG2 antibody 5D3 (2 μg) (Chemicon, Temecula, CA) (*18*) 24 h post-transfection. Cells were then labeled with a FITC-conjugated goat anti-mouse IgG2b secondary antibody (2.5 μg) (Pharmingen, San Diego, CA). Control samples were incubated in parallel with a non-specific isotype-matched control antibody IgG2b (Pharmingen, San Diego, CA).

Fluorescent Substrate Accumulation Assays. Substrate accumulation studies were performed as described previously (*43*). Briefly, HeLa cells were harvested by trypsinization 24 h post-transfection and counted using a Z1 particle counter (Beckman Coulter). Cells (500000) were incubated in media with fluorescent substrates rhodamine 123 (0.5 μg/mL) or mitoxantrone (10 μM) for 30 min at 37 °C to allow for uptake. Cells were then washed and resuspended in drug-free media and incubated for an additional 30 min at 37 °C to promote transporter-mediated efflux. Cellular fluorescence was measured using a FACSCalibur flow cytometer (Becton Dickinson, San Jose, CA) equipped with a 488 nm argon laser and 530 nm band-pass filter (FL1) for rhodamine 123 and a 670 nm band-pass filter (FL3) for mitoxantrone.

ATPase Activity. Vanadate-sensitive ATPase activity analysis was performed as described previously (*43*). Microsomal membranes containing 10 μg of total protein were incubated at 37 °C for 30 min in the presence and absence of 20 μM prazosin and the presence and absence of 300 μM vanadate. ATP hydrolysis was detected by colorimetric detection of inorganic phosphate release.

Chemical Cross-Linking. To cross-link ABCG2 in whole cells, a nonpermeable sulfhydryl-reactive cross-linker, DP-DPB [1,4-di[3′-(2′-pyridyldithio)propionamido]butane (Pierce, Rockford, IL)], was used. The spacer arm of this bifunctional compound has a length of 19.9 Å. Twenty-four hours post-plating, six-well plates containing MCF-7/AdVp3000 cells were incubated with 1 mM DPDPB at 4 °C for 2 h with gentle shaking. The reaction was quenched with the addition of 10 mM cysteine. Cells were subsequently washed, harvested by trypsinization, and lysed in lysis buffer containing 1 mM DTT as described above (see SDS−PAGE and Immunoblot Analysis). SDS−PAGE samples were prepared using an appropriate amount of 5× Laemmli sample buffer without β-ME.

Photoaffinity Nucleotide Cross-Linking. The photoactivatable diazidodiadenine dinucleotide cross-linker, 8-diN_3-AP_4A, was used to cross-link the ATP binding sites (*37*, *38*, *45*). Crude membranes derived from MCF-7/AdVp3000 cells (10−50 μg) were incubated with varying concentrations of 8-diN_3AP_4A (0, 0.25, 0.5, 1.0, 1.5, or 3 mM) for 5−15 min on ice. Specificity control experiments were performed in parallel in the presence of a 10-fold molar excess of ATP. Samples were cross-linked at 365 nm for 20−40 min on ice. SDS−PAGE samples were prepared using an appropriate amount of 5× Laemmli sample buffer containing 3.575 M β-ME.

RESULTS

ABCG2 (R482G) Chimeric Dimers Are Expressed at the Cell Surface and Transport ABCG2 Substrates. To study ABCG2 as a dimer in intact living cells, we constructed artificial chimeric dimers and investigated the localization and activity of these transporters. In all of the experiments presented here involving transient expression of ABCG2, we used the ABCG2 (R482G) variant because it has a broader substrate specificity than the wild-type protein (*39*−*41*, *46*). Throughout, the designation ABCG2 refers to the R482G variant unless otherwise noted. Three chimeric constructs were generated for this study, ABCG2-ABCG2, ABCG2-M-ABCG2, and ABCG2-P-ABCG2. ABCG2-ABCG2 contains two ABCG2 proteins fused directly, separated only by proline−arginine. The other two constructs have a flexible linker region between the two ABCG2 proteins that were derived from either of two full-length ABC transporters, human P-gp or yeast PDR5. The chimeric dimer ABCG2-M-ABCG2 has the linker region (amino acids 633−689) from P-gp (**M**DR1/ABCB1), chosen because it shares many of the same transport substrates as ABCG2. The third construct, ABCG2-P-ABCG2 contains the connecting domain (amino acids 814−883) from **P**DR5, a yeast homologue chosen for its similarity in structural organization to ABCG2. While P-gp has its NBDs on the C-terminal side of the TMDs, the NBDs of PDR5 and ABCG2 are N-terminal to the TMDs.

To evaluate cell surface expression of the ABCG2 chimeric dimers, we used the monoclonal antibody 5D3 that recognizes an external epitope of ABCG2 (*18*). HeLa cells expressing the chimeric dimers were incubated with 5D3 and subsequently incubated with a FITC-conjugate secondary

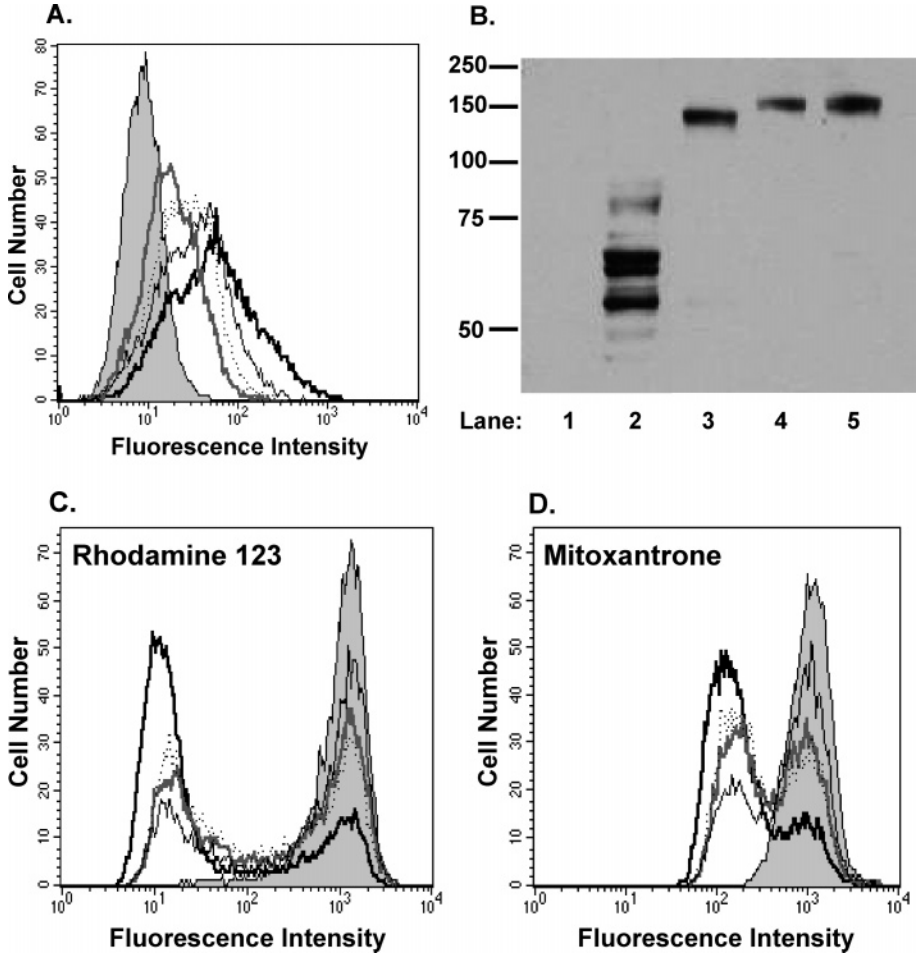

FIGURE 1: Cell surface expression and drug efflux activity of ABCG2 chimeric dimers. (A) Cell surface antibody labeling of ABCG2 and flow cytometric analysis. HeLa cells were co-infected/transfected with plasmid DNA constructs of the empty vector pTM1 (gray shaded peak), ABCG2 (R482G) (black thick line), ABCG2-ABCG2 (gray thick line), ABCG2-M-ABCG2 (black thin line), or ABCG2-P-ABCG2 (dashed line). After 24 h at 32 °C, the cells were harvested by trypsinization and labeled with 5D3, an antibody that recognizes an external epitope of ABCG2. Following antibody labeling, cells were stained with a FITC-conjugated secondary antibody for detection by flow cytometry. (B) Cell surface biotinylation. HeLa cells were co-infected/transfected in six-well plates with plasmid DNA constructs of the empty vector pTM1 (lane 1), ABCG2 (R482G) (lane 2), ABCG2-ABCG2 (lane 3), ABCG2-M-ABCG2 (lane 4), and ABCG2-P-ABCG2 (lane 5). After 24 h at 32 °C, intact adherent cells were incubated with the non-cell-permeable biotinylating agent, sulfo-NHS-biotin (500 μL of 1.5 mg/mL). Cells were washed with buffer containing 100 mM glycine to bind excess biotin prior to cell lysis. Biotinylated proteins were solubilized in RIPA buffer and then selected with monomeric avidin beads. Cell surface proteins were denatured with 1× Laemmli sample buffer containing β-ME, separated by SDS−PAGE (7.5% gel), and detected by immunoblot analysis using the monoclonal antibody BXP-21 (1:1000) as described in Experimental Procedures. (C, D) Drug accumulation in HeLa cells expressing ABCG2 and ABCG2 chimeric dimers. HeLa cells transiently overexpressing various ABCG2 constructs were harvested and incubated in suspension with either (C) rhodamine 123 (0.5 μg/mL) or (D) mitoxantrone (10 μM) for 30 min at 37 °C. Cells were harvested by centrifugation and incubated with drug-free media for an additional 30 min at 37 °C to allow for drug efflux and analyzed by flow cytometry. Histograms depict the cellular fluorescence intensity of the negative control pTM1 empty vector (gray shaded peak), ABCG2 (black thick line), ABCG2-ABCG2 (gray thick line), ABCG2-M-ABCG2 (black thin line), and ABCG2-P-ABCG2 (dashed line).

antibody for detection. All three of the chimeric dimers were expressed at the cell surface compared to the empty vector negative control, as demonstrated by the positive shifts in fluorescence intensity (Figure 1A). Although it appears that these proteins may be expressed to slightly varying degrees on the cell surface, it has recently been shown that the 5D3 antibody is conformation-sensitive (*47*). Therefore, the variations observed between the chimeras may reflect alternative conformations that are differentially recognized by the antibody in addition to actual differences in cell surface expression.

To further confirm expression at the plasma membrane, we performed cell surface biotinylation experiments using the cell-impermeable compound, sulfo-NHS-biotin (Figure 1B). After repeated washing and incubation with 100 mM glycine to remove excess biotin, the labeled plasma membrane proteins were isolated by avidin bead selection and subsequently separated by SDS−PAGE. ABCG2 was detected by immunoblot analysis using the monoclonal antibody BXP-21. This antibody recognizes an internal epitope on the NBD of ABCG2 and has not been shown to be sensitive to conformational differences. To control for specific biotinylation of only plasma membrane proteins, the cytosolic protein GFP was expressed similarly and processed in parallel with the ABCG2 samples. GFP was not biotinylated (data not shown), confirming the specificity of this cell surface assay for plasma membrane proteins under our experimental conditions. Using this assay, all three chimeric dimers and the ABCG2 control were localized to the plasma membrane (Figure 1B). Due to the rapid vaccinia virus-based overexpression system used, monomeric ABCG2 runs as a series of bands between 60 and 80 kDa (Figure 1B, lane 2),

which represents proteins in various glycosylation states (*27*, *48*). The lowest molecular mass band specific for ABCG2 corresponds to the unglycosylated protein that we have recently shown to be expressed at the cell surface (*27*). The chimeric dimers do not show this variability, perhaps due either to uniform glycosylation or to band compression in the higher molecular mass portion of the gel. An alternative explanation is that the dimers are not glycosylated. However, upon treatment of the ABCG2-ABCG2 dimer protein with PNGase F to remove all N-linked glycosylation, a distinct single band was observed at a slightly lower molecular mass, suggesting that this protein is glycosylated uniformly (data not shown). ABCG2-M-ABCG2 (Figure 1B, lane 4) and ABCG2-P-ABCG2 (Figure 1B, lane 5) run at a higher apparent molecular mass on SDS−PAGE than ABCG2-ABCG2 (Figure 1B, lane 3) due to the presence of the linker regions between the two ABCG2 proteins. From these data, it appears that the three chimeric dimers are expressed at similar levels at the cell surface. We cannot, however, compare the expression of the chimeric dimers to the monomeric protein for two reasons. First, the monomeric ABCG2 is expressed as various differentially glycosylated forms, which precludes accurate quantitation. Second, since the chimeric dimers have two epitopes for the BXP-21 antibody, it is possible that multiple antibodies are binding and enhancing the signal. Therefore, it is possible that less protein is being expressed even though the signal strength appears somewhat equivalent.

To determine if the chimeric ABCG2 dimers were functional with respect to drug transport, the various proteins were transiently expressed in HeLa cells using the vaccinia virus expression system. After 24 h at 32 °C, cells were harvested and incubated with the fluorescent ABCG2 (R482G) substrates rhodamine 123 or mitoxantrone for 30 min at 37 °C, followed by a second incubation for 30 min in drug-free media to allow for transporter-mediated efflux. Cellular drug accumulation was analyzed using flow cytometry. Cells transfected with the empty vector, pTM1, serve as the negative control and show the maximum amount of drug accumulation (Figure 1C,D, shaded peak). The transfected monomer ABCG2 shows the greatest decrease in fluorescence intensity, which is indicative of transport (thick black line), for both rhodamine 123 (Figure 1C) and mitoxantrone (Figure 1D). Similar data were obtained for the substrates doxorubicin and daunomycin (data not shown). From these data, we determined that the chimeric dimers transported all ABCG2 substrates examined, albeit to a slightly lesser extent than the monomer-expressed control ABCG2, and the presence of the P-gp or PDR5-derived linker regions between the two ABCG2 monomers was not necessary for activity. It should be noted that the number of cells expressing active transporter, shown by the area under the curves, is lower for all three chimeras compared to the monomer. These data suggest that fewer of the cells are expressing the chimeric dimer at the surface and/or that there are fewer chimeric dimers at the cell surface per cell.

A Single Mutation in the Walker B Motif of ABCG2 (R482G) Monomers and Chimeric Dimers Abrogates Function but Not Cell Surface Expression. To examine the effects of mutations to the ATP binding site on ABCG2 function, we constructed a variant of the monomeric ABCG2 (R482G) in the Walker B motif (D210N), thought to be involved in magnesium binding. This mutation has been shown previously in P-glycoprotein to abrogate function when introduced into either of the NBDs (*30*). We evaluated cell surface expression of ABCG2 (D210N) by flow cytometry using the monoclonal antibody 5D3 that recognizes an external epitope of ABCG2 (*18*), followed by incubation with a FITC-conjugated secondary antibody for detection (Figure 2A), as well as by cell surface biotinylation experiments (Figure 2B). This construct, ABCG2 (D210N), is expressed at the cell surface by both of these assays but is not functional for either rhodamine 123 or mitoxantrone transport (Figure 2C,D). The ABCG2 (D210N) monomer is recognized better by the conformation-sensitive 5D3 antibody than the ABCG2 (R482G) protein, as demonstrated by the greater shift in fluorescence intensity, suggesting that the presence of the mutation may have caused a conformational change in the protein (*47*). We then incorporated this variant into the first gene of the chimeric ABCG2 dimer [ABCG2 (D210N)-ABCG2] and assessed cell surface expression and function by the assays described above. We determined that ABCG2 (D210N)-ABCG2 is expressed at the cell surface by both flow cytometry analysis with the 5D3 antibody (Figure 2A) and cell surface biotinylation (Figure 2B). However, the transport function of this chimera is completely abrogated (Figure 2C,D), showing a pattern similar to both the pTM1 negative control and the ABCG2 (D210N) monomer. These data indicate that two intact ATP sites are necessary for function, as has been established for numerous full-length ABC transporters, and suggest that ABCG2 functions as a dimer. We did not construct the ABCG2 chimeric dimer with the D210N mutation introduced into the second ABCG2 gene, but we predict a similar dominant-negative effect if the protein proved to fold properly.

Nucleotide Cross-Linking of ABCG2 in Cell Membranes Indicates Primarily Dimer Formation. Understanding that ABCG2 can function as a dimer, we investigated potential dimerization interactions. A bifunctional photoactivatable diazidodiadenine dinucleotide cross-linker, 8-diN_3AP_4A, was used to investigate the spatial arrangement of the nucleotide binding domains between monomers of ABCG2, as has been shown previously for a variety of other ATPases and ATP-utilizing enzymes (*37*, *38*, *45*). We hypothesized that ABCG2 monomers will be cross-linked using this ATP analogue if the two NBDs are in close proximity. Because the cross-linker is not cell permeable, these experiments were performed in crude membrane preparations of drug-selected MCF-7/AdVp3000 cells that overexpress a homogeneously glycosylated population of ABCG2 (R482T) (Figure 3A, lane 1). Membrane preparations from these cells were used because of their uniform banding pattern on SDS−PAGE and their high level of ABCG2 (R482T) expression. In the absence of the cross-linker, ABCG2 (R482T) migrates as a monomer by SDS−PAGE analysis (Figure 3A, lane 1). However, in the presence of 8-diN_3AP_4A, the protein migrated to a molecular mass corresponding to the appropriate molecular mass of a dimer (∼150 kDa) in a concentration-dependent manner (Figure 3A, lanes 2−5). While it is possible that the dually modified cross-linker may bind to both NBDs, it is also possible that binding to one NBD will induce the dimerization and the second label will modify a residue outside of the NBD in the second monomer. In the

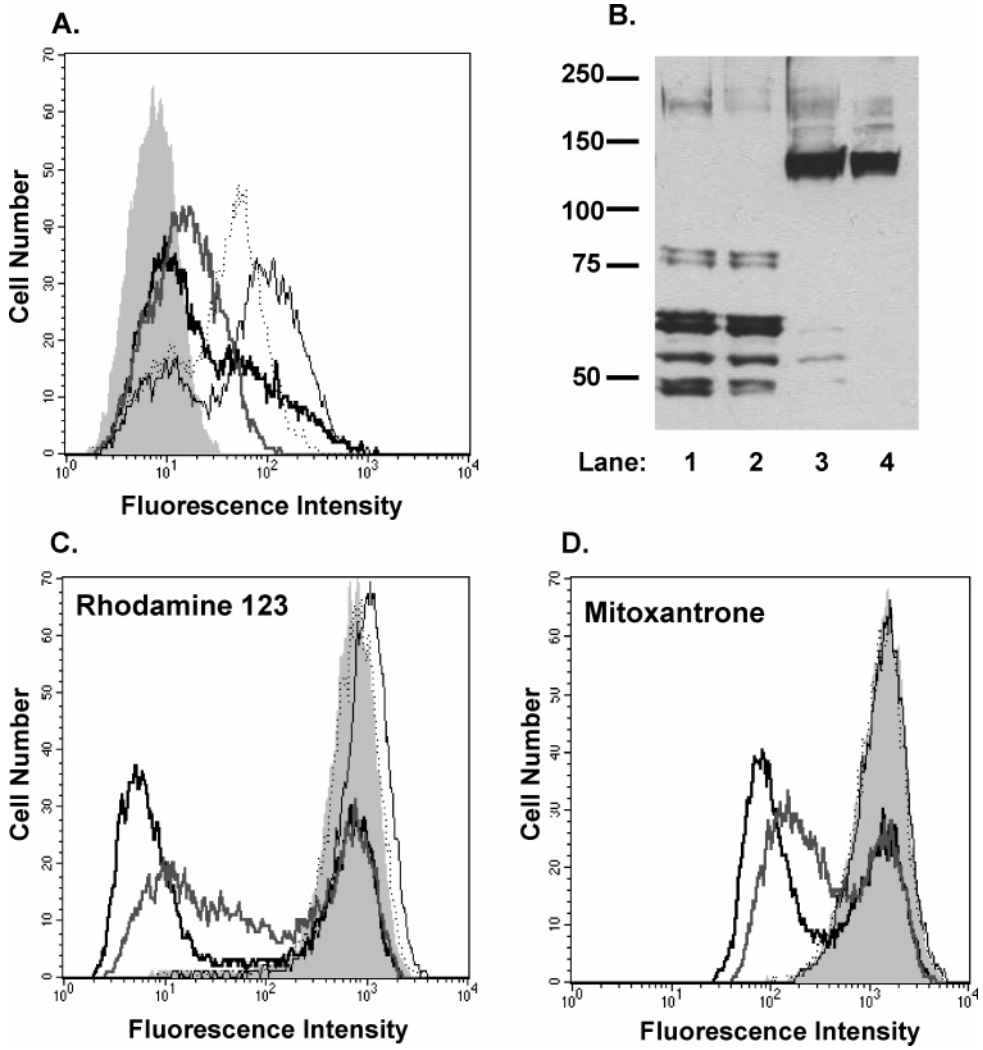

FIGURE 2: Cell surface expression and drug efflux activity of the ABCG2 (D210N) monomer and chimeric dimer ABCG2 (D210N)-ABCG2. (A) Cell surface antibody labeling of ABCG2 and flow cytometric analysis. HeLa cells were co-infected/transfected with plasmid DNA constructs of the empty vector pTM1 (gray shaded peak), ABCG2 (R482G) (black thick line), ABCG2-ABCG2 (gray thick line), ABCG2 (D210N) (black thin line), or ABCG2 (D210N)-ABCG2 (dashed line). After 24 h at 32 °C, the cells were harvested by trypsinization and labeled with 5D3, an antibody that recognizes an external epitope of ABCG2. Following antibody labeling, cells were stained with a FITC-conjugated secondary antibody for detection by flow cytometry. (B) Cell surface biotinylation. HeLa cells were co-infected/transfected in six-well plates with plasmid DNA constructs containing ABCG2 (R482G) (lane 1), ABCG2 (D210N) (lane 2), ABCG2-ABCG2 (lane 3), and ABCG2 (D210N)-ABCG2 (lane 4). After 24 h at 32 °C, intact adherent cells were incubated with the non-cell-permeable biotinylating agent, sulfo-NHS-biotin (500 μL of 1.5 mg/mL). Cells were washed with buffer containing 100 mM glycine to bind excess biotin prior to cell lysis. Biotinylated proteins were solubilized in RIPA buffer and then selected with monomeric avidin beads. Cell surface proteins were denatured with 1× Laemmli sample buffer containing β-ME, separated by SDS−PAGE (7.5% gel), and detected by immunoblot analysis using the monoclonal antibody BXP-21 (1:1000) as described in Experimental Procedures. (C, D) Drug accumulation in HeLa cells expressing the ABCG2 (D210N) monomer and chimeric dimer. HeLa cells transiently overexpressing various ABCG2 constructs were harvested and incubated in suspension with either (C) rhodamine 123 (0.5 μg/mL) or (D) mitoxantrone (10 μM) for 30 min at 37 °C. Cells were harvested by centrifugation and incubated with drug-free media for an additional 30 min at 37 °C to allow for drug efflux and analyzed by flow cytometry. Histograms depict the cellular fluorescence intensity of the negative control pTM1 empty vector (gray shaded peak), ABCG2 (black thick line), ABCG2-ABCG2 (gray thick line), ABCG2 (D210N) (black thin line), and ABCG2 (D210N)-ABCG2 (dashed line).

presence of 1.5 or 3 mM 8-diN_3AP_4A, although the predominant form observed is the dimer, a higher molecular mass complex is visualized in addition to the dimer band (Figure 3A, lane 5, and Figure 3B, lane 2), suggesting the presence of either a higher order oligomer or, possibly, an aggregate. To ensure that the cross-linking was specific for one or both of the nucleotide binding domains, parallel experiments were performed in the presence of a 10-fold molar excess of ATP, the largest excess amount allowed by our assay conditions (Figure 3B, lane 3). Under these conditions, the presence of dimers and higher molecular mass species was markedly reduced, suggesting that, for the most part, ATP competed specifically and effectively for the NBD in the dimers/oligomers.

Cysteine Cross-Linking of ABCG2 in Whole Cells Suggests the Presence of a Dimer. To investigate the formation of ABCG2 oligomers under more physiologically relevant conditions, we performed chemical cross-linking experiments in intact live cells. There are three extracellular cysteine residues in the third predicted extracellular loop of ABCG2 (*2*, *3*). Therefore, we used the non-membrane-permeable bifunctional sulfhydryl-reactive cross-linker DPDPB [1,4-di[3′-(2′-pyridyldithio)propionamido]butane] that has a spacer length of 19.9 Å (*49*) to determine if these extracellular

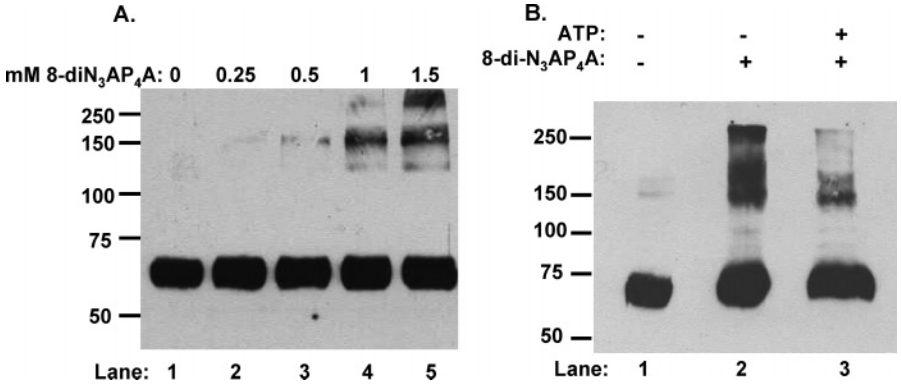

FIGURE 3: Nucleotide cross-linking of ABCG2 (R482T) in cell membranes. (A) Crude membrane preparations from MCF-7/AdVp3000 cells (10 μg) were incubated for 20 min on ice with increasing concentrations of 8-diN$_3$AP$_4$A under UV light (365 nm): lane 1, 0 mM; lane 2, 0.25 mM; lane 3, 0.5 mM; lane 4, 1.0 mM; lane 5, 1.5 mM. (B) Crude membranes preparations from MCF-7/AdVp3000 cells (50 μg) were incubated for 40 min on ice in the presence (lanes 2 and 3) or absence (lane 1) of 3 mM 8-diN$_3$AP$_4$A and in the presence (lane 3) or absence (lanes 1 and 2) of 30 mM ATP. Proteins (5 μg in panel B and 25 μg in panel C) were separated by SDS−PAGE (7.5% gel) and detected by immunoblot analysis using the monoclonal antibody BXP-21 (1:1000) as described in Experimental Procedures.

cysteines can participate in disulfide linkages to form dimers of ABCG2 in whole cells. In six-well plates, MCF-7/AdVp3000 cells overexpressing ABCG2 (R482T) were incubated with a 1 mM solution of DPDPB for 2 h at 4 °C. The cross-linking reaction was stopped by the addition of a 10-fold molar excess of cysteine (10 mM). The cells were harvested by trypsinization and lysed in the presence of 1 mM DTT. The proteins were separated by SDS−PAGE in the absence of β-ME to reveal cross-linked species. Given that the bifunctional cross-linker is sensitive to reduction by thiols, we omitted β-ME in the SDS−PAGE sample buffer. However, we found that, under our experimental conditions, the addition of 1 mM DTT in the lysis buffer prevents nonspecific dimer formation involving other cysteines in the protein that is often observed in the total absence of reducing agent (refs *4* and *5* and this study). When ABCG2 (R482T) was cross-linked with DPDPB, a higher molecular mass species at a molecular mass consistent with an ABCG2 (R482T) dimer (Figure 4, lane 2) was apparent, as compared to the monomer species observed in the absence of the cross-linker (Figure 4, lane 1). As a further control for specificity, we produced a variant of ABCG2 in which the cysteines were replaced with alanines (ABCG2ΔEC-C) and transiently expressed the protein in HeLa cells. Under conditions similar to those described above, no dimer or higher order oligomer formation was observed using the extracellular cysteine-less variant (data not shown). Together, these data provide support for the hypothesis that the third extracellular loops of distinct ABCG2 monomers are spatially proximal and the cysteines within those loops may form disulfide linkages in whole cells. We also observe higher molecular mass species in the cross-linked sample, consistent with higher order oligomers or aggregates.

The Extracellular Cysteine-less ABCG2 Variant Is Expressed at the Cell Surface and Retains both Drug Transport and ATPase Activities. To investigate whether extracellular disulfide bond formation is necessary for dimerization and function, we determined the cellular localization and functional status of the variant ABCG2ΔEC-C described above, which has the three extracellular cysteine residues replaced with alanines. This variant was not recognized by the 5D3 antibody (data not shown), suggesting that the third extracellular loop and, perhaps, the cysteines themselves comprise

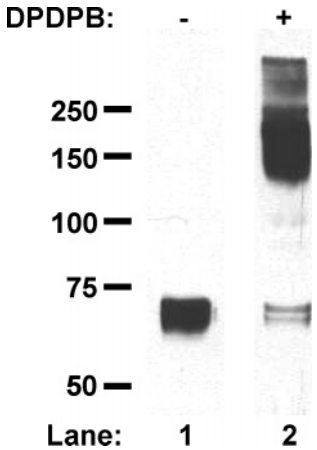

FIGURE 4: Sulfhydryl-reactive chemical cross-linking of ABCG2 (R482T) in whole cells. In a six-well plate, MCF-7/AdVp3000 cells expressing ABCG2 were incubated in the absence (lane 1) or presence (lane 2) of the sulfhydryl-reactive non-cell-permeable cross-linker DPDPB (1 mM in 10% DMSO) for 2 h at 4 °C. Chemical cross-linking was stopped by washing excess surface DPDPB away and quenching with buffer containing 10 mM cysteine. Cells were lysed in lysis buffer containing 1 mM DTT and proteins solubilized with an appropriate amount of 5× SDS sample buffer without β-ME. Proteins were separated by SDS−PAGE (7.5% gel) and detected by immunoblot analysis using the monoclonal antibody BXP-21 (1:1000) as described in Experimental Procedures.

at least part of the epitope for the antibody or that the protein has an altered conformation such that it is no longer recognized by the antibody. Therefore, we performed cell surface biotinylation experiments using sulfo-NHS-biotin as described above for the chimeric dimers and demonstrated that ABCG2ΔEC-C was expressed at the plasma membrane in whole cells (Figure 5A, lane 3) similar to the ABCG2 control (Figure 5A, lane 2). In addition, using the monoclonal antibody BXP-21 in permeabilized cells, the ABCG2ΔEC-C variant was determined to be present at the cell surface in a manner indistinguishable from the ABCG2 control by confocal microscopy (data not shown).

To determine if the extracellular cysteine residues are crucial for activity, the ABCG2ΔEC-C variant was expressed in HeLa cells, and drug transport activity was measured as described in Experimental Procedures. We observed that the ABCG2ΔEC-C variant had comparable levels of transport

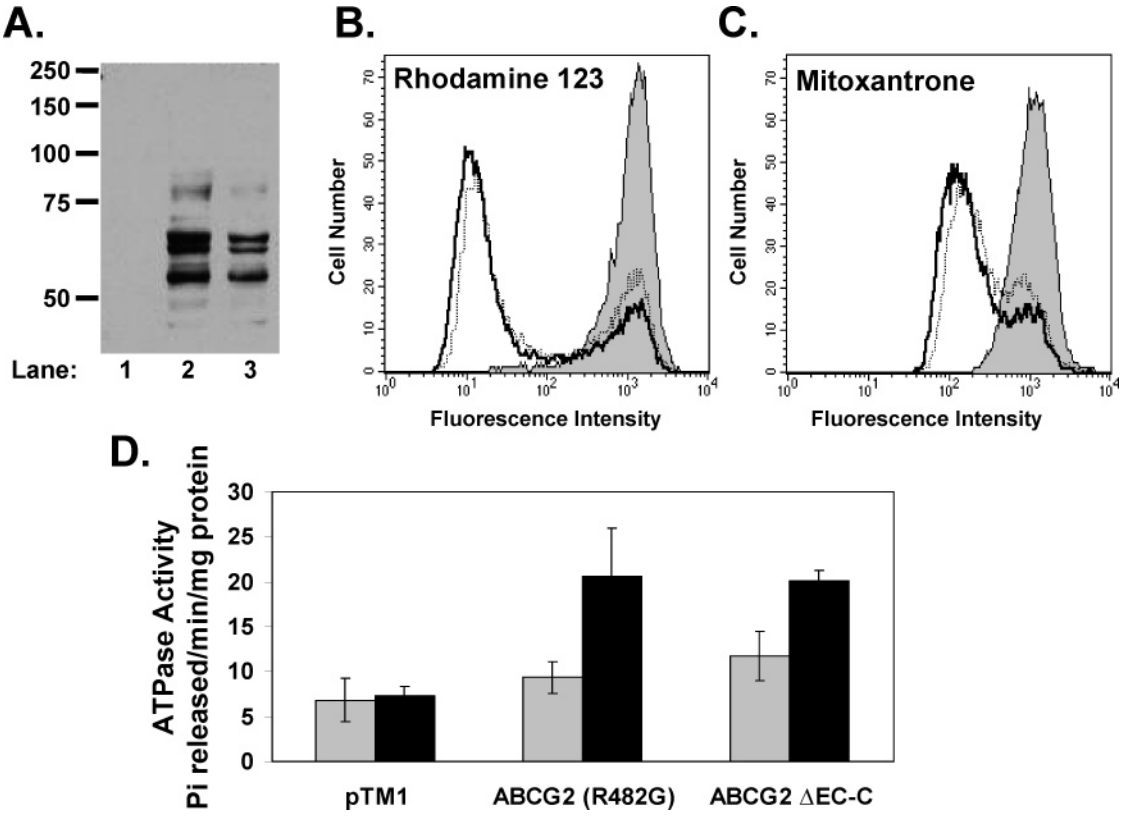

FIGURE 5: Characterization of the ABCG2 extracellular cysteine-less (ABCG2ΔEC-C) variant transiently expressed in HeLa cells. (A) Cell surface expression of ABCG2ΔEC-C determined by biotinylation as described in Experimental Procedures. HeLa cells in six-well plates were transfected with plasmid DNA constructs of the empty vector pTM1 (lane 1), ABCG2 (lane 2), and ABCG2ΔEC-C (lane 3). Cells were incubated with the non-cell-permeable biotinylating agent, sulfo-NHS-biotin (500 μL of 1.5 mg/mL). Cells were washed with buffer containing 100 mM glycine to bind excess biotin prior to cell lysis. Biotinylated proteins were solubilized with RIPA buffer and selected with monomeric avidin beads. Cell surface proteins were denatured with 1× SDS sample buffer containing β-ME, separated by SDS−PAGE (7.5% gel), and detected by immunoblot analysis using the monoclonal antibody BXP-21 (1:1000) as described in Experimental Procedures. (B, C) Fluorescent drug accumulation of ABCG2-expressing cells. HeLa cells overexpressing ABCG2 or ABCG2ΔEC-C were harvested and incubated with either (B) rhodamine 123 (0.5 μg/mL) or (C) mitoxantrone (10 μM). Cells were washed and incubated with drug-free media to allow for drug efflux and then analyzed by flow cytometry. Histograms depict the cellular fluorescence intensity of the empty vector negative control (gray shaded peak), ABCG2 (black thick line), and ABCG2ΔEC-C (dashed line). (D) ATPase activity of crude membrane preparations from ABCG2-expressing cells. Basal (gray bars) and drug-stimulated ATPase activity (black bars) of pTM1 (negative control empty vector), ABCG2 (R482), and ABCG2ΔEC-C in the ABCG2 (R482G) background. Vanadate-sensitive ATP hydrolysis was measured in crude membrane preparations from transfected HeLa cells stimulated in the presence and absence of 20 μM prazosin. Basal activity measurements represent the vanadate-sensitive ATP hydrolysis in the absence of drug stimulation. Assays were performed with 10 μg of total membrane protein in quadruplicate and repeated a minimum of three times.

for rhodamine 123 (Figure 5B, dashed line), mitoxantrone (Figure 5C, dashed line), daunomycin (data not shown), and doxorubicin (data not shown) as compared to ABCG2 (Figure 5B and C, thick line). As an additional measure of transporter activity, we measured both the vanadate-sensitive basal and drug-stimulated ATPase activity of the ABCG2ΔEC-C variant. Crude HeLa cell membrane preparations of cells transiently overexpressing the ABCG2 and ABCG2ΔEC-C were incubated in the presence (stimulated) and absence (basal) of 20 μM ABCG2 (R482G) substrate prazosin. The ABCG2ΔEC-C variant demonstrated drug-stimulated ATPase activity comparable to the parent protein, ABCG2 (R482G), with perhaps a slight increase in the basal activity (Figure 5D). Taken together with the fact that the 5D3 antibody did not recognize ABCG2ΔEC-C, these data demonstrate that the absence of the extracellular cysteine residues in ABCG2 may cause a conformational change in the protein but does not prevent the proper cellular localization or the overall function of ABCG2, further suggesting that the formation of an extracellular disulfide bond between monomers, while possible, is not critical to dimerization.

DISCUSSION

The aims of this study were to characterize the dimerization/oligomerization of ABCG2 and to investigate the relevance of potential disulfide bonds in the dimerization/oligomerization. It is widely accepted that ABCG2 is likely to function as a dimer or higher order oligomer (*4*, *5*, *26*, *50*), and we provide here direct evidence that ABCG2 can function as a dimer. By expressing covalent dimers, we determined that these ABCG2 molecules retain their localization to the plasma membrane and their drug transport activity. Although the ABCG2 dimers that were tethered via a flexible linker domain were functional, we also found that the dimer made by fusing two ABCG2 genes directly was functional. These data are in contrast to P-gp, where it was found that disruption of the linker region joining the two intact halves of the protein eliminates drug transport as well as ATPase activity (*51*). The differences in the location of the NBDs with respect to the TMDs may account for this dissimilarity. Each half of PDR5 has similar topology to ABCG2, but the two halves are also connected by a flexible

linker domain. Our data suggest that the linker domain of PDR5 may not be essential for the interaction of the two halves of the protein but may serve another function. We also demonstrated that inactivation of one of the ABCG2 proteins in the chimeric dimer abrogates function, further supporting our hypothesis that ABCG2 functions as a dimer. These data are corroborated by two studies that demonstrated co-immunoprecipitation of differentially tagged ABCG2 monomers (*5*, *26*), including dominant-negative effects upon coexpression of wild-type ABCG2 and inactive ABCG2 molecules containing a Walker A mutation (K86M) (*26*) or a Leu to Pro mutation in the fifth transmembrane segment at position 554 (*5*). However, the K86M mutation appears to have a more dramatic effect on targeting of ABCG2 to the cell surface than the D210N mutation described here. By cell surface biotinylation experiments, we showed that ABCG2 (D210N) is expressed at the surface similarly to ABCG2 (R482G) (Figure 2B) whereas ABCG2 (K86M) is found predominantly in the endoplasmic reticulum with a small percentage localized to the plasma membrane (*26*).

In addition, we also investigated which segments of the transporter may be in close proximity in the dimer state. Both structural and biochemical studies on full-length and bacterial oligomeric ABC transporters have demonstrated that the two NBDs are in close proximity and, in fact, physically interact and hydrolyze ATP in a coordinated manner (*30*, *32*−*34*, *36*, *51*−*60*). In addition, it has been shown that ATP binding induces dimerization of the yeast mitochondrial ABC transporter Mdl1p (*23*), MJ0796 (*35*, *36*), and the ABC transporter-related protein Rad50 (*61*). We show here, using photoaffinity cross-linking with a bifunctional diazidodiadenine dinucleotide cross-linker that the NBDs of ABCG2 are closely associated in an ABCG2 dimer/oligomer. The cross-linked complex appears to be a dimer of ABCG2 or, perhaps, a higher order oligomer at higher concentrations of the photoaffinity label. Taken together, our data suggest that a major functional interface between the monomers involves these domains. In addition, ABCG2 will likely follow the model of other ABC transporters where at least one bound ATP is shared between the two NBDs and that the NBDs function in a coordinated fashion.

It has been previously shown that chemical cross-linking of ABCG2 using a lipid-permeable amine-reactive cross-linking agent can produce a dimer or higher order oligomer as visualized by SDS−PAGE in live cells, thereby implicating extracellular, intramembrane, and intracellular amino acids (*4*, *6*, *62*). In this study, by using intact cells and a non-lipid-permeable sulfhydryl-specific cross-linking agent, we established that the third cysteine-containing extracellular loop is involved in the cross-linked dimer through the formation of a disulfide bridge, suggesting that these regions are also close to each other in the native cellular environment. Furthermore, we demonstrated that the absence of the cysteine residues, and thus the disulfide bridge between the third extracellular loops of monomers, had little to no effect on either the localization or the activity of the transporter, suggesting that the protein was in its proper oligomeric state. These data demonstrate that the functional transporter does not necessarily need an extracellular disulfide bridge for function and/or oligomerization, but the proximity of the third extracellular loop domains in space suggests that one or more may exist in vivo.

It is likely that we will identify interactions between the TMDs from individual ABCG2 monomers that will form substrate binding sites. Disulfide cross-linking and cysteine-scanning mutagenesis have been used successfully to determine which TMDs of P-glycoprotein are close together (*63*−*68*) as well as to develop an atomic detail model of the transporter (*69*). In addition, similar cysteine-scanning mutagenesis experiments have also been performed on the soluble and membrane domains of the bacterial ABC transporter LmrA (*70*). Because these experiments necessitate the generation of a completely cysteine-less variant of the transporter, these experiments have yet to be performed with ABCG2. Our laboratory is in the process of generating this construct, using the functional ABCG2ΔEC-C variant as a starting point.

Various studies, including the work presented here, implicate several areas of interaction between monomeric subunits including the GXXXG motif in the first transmembrane domain (*62*), the third extracellular loop, and the nucleotide binding domain. A more definitive and complete understanding of the oligomerization state of ABCG2 will come upon full purification and reconstitution of active ABCG2 followed by analytical ultracentrifugation and/or structural studies by electron microscopy or three-dimensional crystallography.

The minimal functional unit for all of the known eukaryotic ABC transporters to date is two NBDs and two transmembrane domains; however, association of these units into higher order structures remains controversial. Conflicting reports for the existence of P-gp monomers (*60*, *71*) versus dimers (*72*−*76*) have been published in recent years, although the data suggesting the monomer form are from more direct structural findings rather than biochemical work. MRP1, on the other hand, has been shown structurally and biochemically to exist as a dimer (*77*, *78*). Our work and other studies (*5*, *26*, *62*) suggest that the major oligomeric ABCG2 species is a dimer, although at this time we cannot rule out the possibility of higher order oligomers forming in vivo as suggested by Xu et al. (*4*).

The pivotal role of ABCG2 in the gut, the blood brain barrier, stem cells, and the placenta (*3*, *13*, *15*, *79*−*82*) suggests that inhibition of this drug transporter may be an attractive way to increase the transport of chemotherapeutic agents into the bloodstream, the placenta, and the brain. The development of effective, reversible, nontoxic inhibitors of ABCG2 to be used in combination with currently used therapeutic agents would result in improved bioavailability and thus improved clinical efficacy of these treatments. To date, few compounds, vanadate for example, have been developed that inhibit the catalytic activity of ABC transporters directly. In fact, most inhibitors/reversing agents of P-gp are simply competitive substrates for the transporter (*83*). Recently, however, polyvalent stipiamide dimers have been shown to reverse drug resistance in cell lines overexpressing P-gp (*84*, *85*) that may be acting more as true inhibitors of P-gp by binding to the active site but not being transported themselves. Numerous biochemical studies have indicated that drug transport in P-gp is intimately coupled to ATPase activity and correct association of the ATPase domains is essential for transport (reviewed in refs *2*, *3*, *8*, and *83*). An alternative strategy, therefore, would be to specifically block or disrupt the association of the two NBDs of ABCG2 or

other ABC transporters. Therefore, understanding the molecular structure of the ABCG2 dimer interface would be important for the development of inhibitors using rational structure-based drug design approaches.

ACKNOWLEDGMENT

We thank Vicki L. Croy for cell culture work, Christa L. Feasley for the construction of chimeric dimer plasmids, and Karin F. K. Ejendal for the preparation of crude membranes and critical reading of the manuscript.

REFERENCES

1. Rocchi, E., Khodjakov, A., Volk, E. L., Yang, C. H., Litman, T., Bates, S. E., and Schneider, E. (2000) The product of the ABC half-transporter gene ABCG2 (BCRP/MXR/ABCP) is expressed in the plasma membrane, *Biochem. Biophys. Res. Commun. 271*, 42−46.
2. Ejendal, K. F., and Hrycyna, C. A. (2002) Multidrug resistance and cancer: the role of the human ABC transporter ABCG2, *Curr. Protein Pept. Sci. 3*, 503−511.
3. Sarkadi, B., Ozvegy-Laczka, C., Nemet, K., and Varadi, A. (2004) ABCG2−a transporter for all seasons, *FEBS Lett. 567*, 116−120.
4. Xu, J., Liu, Y., Yang, Y., Bates, S., and Zhang, J. T. (2004) Characterization of oligomeric human half-ABC transporter ATP-binding cassette G2, *J. Biol. Chem. 279*, 19781−19789.
5. Kage, K., Tsukahara, S., Sugiyama, T., Asada, S., Ishikawa, E., Tsuruo, T., and Sugimoto, Y. (2002) Dominant-negative inhibition of breast cancer resistance protein as drug efflux pump through the inhibition of S-S dependent homodimerization, *Int. J. Cancer 97*, 626−630.
6. Litman, T., Jensen, U., Hansen, A., Covitz, K. M., Zhan, Z., Fetsch, P., Abati, A., Hansen, P. R., Horn, T., Skovsgaard, T., and Bates, S. E. (2002) Use of peptide antibodies to probe for the mitoxantrone resistance-associated protein MXR/BCRP/ABCP/ABCG2, *Biochim. Biophys. Acta 1565*, 6−16.
7. Hrycyna, C. A. (2001) Molecular genetic analysis and biochemical characterization of mammalian P-glycoproteins involved in multidrug resistance, *Semin. Cell Dev. Biol. 12*, 247−256.
8. Gottesman, M. M., and Pastan, I. (1993) Biochemistry of multidrug resistance mediated by the multidrug transporter, *Annu. Rev. Biochem. 62*, 385−427.
9. Gottesman, M. M., Fojo, T., and Bates, S. E. (2002) Multidrug resistance in cancer: role of ATP-dependent transporters, *Nat. Rev. Cancer 2*, 48−58.
10. Allikmets, R., Schriml, L. M., Hutchinson, A., Romano-Spica, V., and Dean, M. (1998) A human placenta-specific ATP-binding cassette gene (ABCP) on chromosome 4q22 that is involved in multidrug resistance, *Cancer Res. 58*, 5337−5339.
11. Miyake, K., Mickley, L., Litman, T., Zhan, Z., Robey, R., Cristensen, B., Brangi, M., Greenberger, L., Dean, M., Fojo, T., and Bates, S. E. (1999) Molecular cloning of cDNAs which are highly overexpressed in mitoxantrone-resistant cells: demonstration of homology to ABC transport genes, *Cancer Res. 59*, 8−13.
12. Doyle, L. A., Yang, W., Abruzzo, L. V., Krogmann, T., Gao, Y., Rishi, A. K., and Ross, D. D. (1998) A multidrug resistance transporter from human MCF-7 breast cancer cells, *Proc. Natl. Acad. Sci. U.S.A. 95*, 15665−15670.
13. Cisternino, S., Mercier, C., Bourasset, F., Roux, F., and Scherrmann, J. M. (2004) Expression, up-regulation, and transport activity of the multidrug-resistance protein Abcg2 at the mouse blood-brain barrier, *Cancer Res. 64*, 3296−3301.
14. Allikmets, R., and Dean, M. (1998) Cloning of novel ABC transporter genes, *Methods Enzymol. 292*, 116−130.
15. Maliepaard, M., Scheffer, G. L., Faneyte, I. F., van Gastelen, M. A., Pijnenborg, A. C., Schinkel, A. H., van De Vijver, M. J., Scheper, R. J., and Schellens, J. H. (2001) Subcellular localization and distribution of the breast cancer resistance protein transporter in normal human tissues, *Cancer Res. 61*, 3458−3464.
16. Jonker, J. W., Smit, J. W., Brinkhuis, R. F., Maliepaard, M., Beijnen, J. H., Schellens, J. H., and Schinkel, A. H. (2000) Role of breast cancer resistance protein in the bioavailability and fetal penetration of topotecan, *J. Natl. Cancer Inst. 92*, 1651−1656.
17. Taipalensuu, J., Tornblom, H., Lindberg, G., Einarsson, C., Sjoqvist, F., Melhus, H., Garberg, P., Sjostrom, B., Lundgren, B., and Artursson, P. (2001) Correlation of gene expression of ten drug efflux proteins of the ATP-binding cassette transporter family in normal human jejunum and in human intestinal epithelial Caco-2 cell monolayers, *J. Pharmacol. Exp. Ther. 299*, 164−170.
18. Zhou, S., Schuetz, J. D., Bunting, K. D., Colapietro, A. M., Sampath, J., Morris, J. J., Lagutina, I., Grosveld, G. C., Osawa, M., Nakauchi, H., and Sorrentino, B. P. (2001) The ABC transporter Bcrp1/ABCG2 is expressed in a wide variety of stem cells and is a molecular determinant of the side-population phenotype, *Nat. Med. 7*, 1028−1034.
19. Liu, L. X., Janvier, K., Berteaux-Lecellier, V., Cartier, N., Benarous, R., and Aubourg, P. (1999) Homo- and heterodimerization of peroxisomal ATP-binding cassette half-transporters, *J. Biol. Chem. 274*, 32738−32743.
20. Vos, J. C., Reits, E. A., Wojcik-Jacobs, E., and Neefjes, J. (2000) Head-head/tail-tail relative orientation of the pore-forming domains of the heterodimeric ABC transporter TAP, *Curr. Biol. 10*, 1−7.
21. Graf, G. A., Yu, L., Li, W. P., Gerard, R., Tuma, P. L., Cohen, J. C., and Hobbs, H. H. (2003) ABCG5 and ABCG8 are obligate heterodimers for protein trafficking and biliary cholesterol excretion, *J. Biol. Chem. 278*, 48275−48282.
22. Graf, G. A., Cohen, J. C., and Hobbs, H. H. (2004) Missense mutations in ABCG5 and ABCG8 disrupt heterodimerization and trafficking, *J. Biol. Chem. 279*, 24881−24888.
23. Janas, E., Hofacker, M., Chen, M., Gompf, S., van der Does, C., and Tampe, R. (2003) The ATP hydrolysis cycle of the nucleotide-binding domain of the mitochondrial ATP-binding cassette transporter Mdl1p, *J. Biol. Chem. 278*, 26862−26869.
24. Yoshikawa, M., Kasamatsu, S., Yasunaga, M., Wang, G., Ikegami, Y., Yoshida, H., Tarui, S., Yabuuchi, H., and Ishikawa, T. (2002) Does ABCG2 need a heterodimer partner? Expression and functional evaluation of ABCG2 (Arg 482), *Drug Metab. Pharmacokinet. 17*, 130−135.
25. Bates, S. E., Robey, R., Miyake, K., Rao, K., Ross, D. D., and Litman, T. (2001) The role of half-transporters in multidrug resistance, *J. Bioenerg. Biomembr. 33*, 503−511.
26. Henriksen, U., Gether, U., and Litman, T. (2005) Effect of Walker A mutation (K86M) on oligomerization and surface targeting of the multidrug resistance transporter ABCG2, *J. Cell Sci. 118*, 1417−1426.
27. Diop, N. K., and Hrycyna, C. A. (2005) N-Linked glycosylation of the human ABC transporter ABCG2 on asparagine 596 is not essential for expression, transport activity, or trafficking to the plasma membrane, *Biochemistry 44*, 5420−5429.
28. Janvilisri, T., Venter, H., Shahi, S., Reuter, G., Balakrishnan, L., and van Veen, H. W. (2003) Sterol transport by the human breast cancer resistance protein (ABCG2) expressed in *Lactococcus lactis*, *J. Biol. Chem. 278*, 20645−20651.
29. Hrycyna, C. A. (1998) Multidrug ABC transporters from bacteria to man: an emerging hypothesis for the universality of molecular mechanism and function, *Drug Resistance Updates 1*, 81−83.
30. Hrycyna, C. A., Ramachandra, M., Germann, U. A., Cheng, P. W., Pastan, I., and Gottesman, M. M. (1999) Both ATP sites of human P-glycoprotein are essential but not symmetric, *Biochemistry 38*, 13887−13899.
31. Urbatsch, I. L., Sankaran, B., Bhagat, S., and Senior, A. E. (1995) Both P-glycoprotein nucleotide-binding sites are catalytically active, *J. Biol. Chem. 270*, 26956−26961.
32. Loo, T. W., and Clarke, D. M. (1995) Covalent modification of human P-glycoprotein mutants containing a single cysteine in either nucleotide-binding fold abolishes drug-stimulated ATPase activity, *J. Biol. Chem. 270*, 22957−22961.
33. Muller, M., Bakos, E., Welker, E., Varadi, A., Germann, U. A., Gottesman, M. M., Morse, B. S., Roninson, I. B., and Sarkadi, B. (1996) Altered drug-stimulated ATPase activity in mutants of the human multidrug resistance protein, *J. Biol. Chem. 271*, 1877−1883.
34. Azzaria, M., Schurr, E., and Gros, P. (1989) Discrete mutations introduced in the predicted nucleotide-binding sites of the mdr1 gene abolish its ability to confer multidrug resistance, *Mol. Cell. Biol. 9*, 5289−5297.
35. Smith, P. C., Karpowich, N., Millen, L., Moody, J. E., Rosen, J., Thomas, P. J., and Hunt, J. F. (2002) ATP binding to the motor domain from an ABC transporter drives formation of a nucleotide sandwich dimer, *Mol. Cell 10*, 139−149.

36. Moody, J. E., Millen, L., Binns, D., Hunt, J. F., and Thomas, P. J. (2002) Cooperative, ATP-dependent association of the nucleotide binding cassettes during the catalytic cycle of ATP-binding cassette transporters, *J. Biol. Chem. 277*, 21111−21114.
37. Schäfer, H.-J. (1986) Divalent azido-ATP analog for photoaffinity cross-linking of F1 subunits, *Methods Enzymol. 126*, 649−660.
38. Knoche, M., Mönnich, K., Schäfer, H.-J., and Kopperschläger, G. (2001) Photoaffinity labeling and photoaffinity cross-linking of phosphofructokinase-1 from *Saccharomyces cerevisiae* by 8-azidoadeninenucleotides, *Arch. Biochem. Biophys. 385*, 301−310.
39. Honjo, Y., Hrycyna, C. A., Yan, Q. W., Medina-Perez, W. Y., Robey, R. W., van De Laar, A., Litman, T., Dean, M., and Bates, S. E. (2001) Acquired mutations in the mxr/bcrp/abcp gene alter substrate specificity in mxr/bcrp/abcp-overexpressing cells, *Cancer Res. 61*, 6635−6639.
40. Miwa, M., Tsukahara, S., Ishikawa, E., Asada, S., Imai, Y., and Sugimoto, Y. (2003) Single amino acid substitutions in the transmembrane domains of breast cancer resistance protein (BCRP) alter cross resistance patterns in transfectants, *Int. J. Cancer 107*, 757−763.
41. Robey, R. W., Honjo, Y., Morisaki, K., Nadjem, T. A., Runge, S., Risbood, M., Poruchynsky, M. S., and Bates, S. E. (2003) Mutations at amino-acid 482 in the ABCG2 gene affect substrate and antagonist specificity, *Br. J. Cancer 89*, 1971−1978.
42. Maliepaard, M., van Gastelen, M. A., de Jong, L. A., Pluim, D., van Waardenburg, R. C., Ruevekamp-Helmers, M. C., Floot, B. G., and Schellens, J. H. (1999) Overexpression of the BCRP/MXR/ABCP gene in a topotecan-selected ovarian tumor cell line, *Cancer Res. 59*, 4559−4563.
43. Hrycyna, C. A., Ramachandra, M., Pastan, I., and Gottesman, M. M. (1998) Functional expression of human P-glycoprotein from plasmids using vaccinia virus-bacteriophage T7 RNA polymerase system, *Methods Enzymol. 292*, 456−473.
44. Laemmli, U. K. (1970) Cleavage of structural proteins during the assembly of the head of bacteriophage T4, *Nature 227*, 680−685.
45. Schäfer, H.-J., and Schuhen, A. (1996) Photoaffinity labeling and photoaffinity cross-linking of enzymes, *Biol. Res. 29*, 31−46.
46. Özvegy, C., Varadi, A., and Sarkadi, B. (2002) Characterization of drug transport, ATP hydrolysis, and nucleotide trapping by the human ABCG2 multidrug transporter. Modulation of substrate specificity by a point mutation, *J. Biol. Chem. 277*, 47980−47990.
47. Ozvegy-Laczka, C., Varady, G., Koblos, G., Ujhelly, O., Cervenak, J., Schuetz, J. D., Sorrentino, B. P., Koomen, G. J., Varadi, A., Nemet, K., and Sarkadi, B. (2005) Function-dependent conformational changes of the ABCG2 multidrug transporter modify its interaction with a monoclonal antibody on the cell surface, *J. Biol. Chem. 280*, 4219−4227.
48. Ejendal, K. F., and Hrycyna, C. A. (2005) Differential sensitivities of the human ATP-binding cassette transporters ABCG2 and P-glycoprotein to cyclosporin A, *Mol. Pharmacol. 67*, 902−911.
49. Zecherle, G. N., Oleinikov, A., and Traut, R. R. (1992) The proximity of the C-terminal domain of *Escherichia coli* ribosomal protein L7/L12 to L10 determined by cysteine site-directed mutagenesis and protein−protein cross-linking, *J. Biol. Chem. 267*, 5889−5896.
50. Litman, T., Brangi, M., Hudson, E., Fetsch, P., Abati, A., Ross, D. D., Miyake, K., Resau, J. H., and Bates, S. E. (2000) The multidrug-resistant phenotype associated with overexpression of the new ABC half-transporter, MXR (ABCG2), *J. Cell. Sci. 113* (Part 11), 2011−2021.
51. Hrycyna, C. A., Airan, L. E., Germann, U. A., Ambudkar, S. V., Pastan, I., and Gottesman, M. M. (1998) Structural flexibility of the linker region of human P-glycoprotein permits ATP hydrolysis and drug transport, *Biochemistry 37*, 13660−13673.
52. Hrycyna, C. A., Ramachandra, M., Ambudkar, S. V., Ko, Y. H., Pedersen, P. L., Pastan, I., and Gottesman, M. M. (1998) Mechanism of action of human P-glycoprotein ATPase activity. Photochemical cleavage during a catalytic transition state using orthovanadate reveals cross-talk between the two ATP sites, *J. Biol. Chem. 273*, 16631−16634.
53. Loo, T. W., and Clarke, D. M. (1995) Rapid purification of human P-glycoprotein mutants expressed transiently in HEK 293 cells by nickel-chelate chromatography and characterization of their drug-stimulated ATPase activities, *J. Biol. Chem. 270*, 21449−21452.
54. Qu, Q., and Sharom, F. J. (2001) FRET analysis indicates that the two ATPase active sites of the P-glycoprotein multidrug transporter are closely associated, *Biochemistry 40*, 1413−1422.
55. Urbatsch, I. L., Sankaran, B., Weber, J., and Senior, A. E. (1995) P-glycoprotein is stably inhibited by vanadate-induced trapping of nucleotide at a single catalytic site, *J. Biol. Chem. 270*, 19383−19390.
56. Urbatsch, I. L., Beaudet, L., Carrier, I., and Gros, P. (1998) Mutations in either nucleotide-binding site of P-glycoprotein (Mdr3) prevent vanadate trapping of nucleotide at both sites, *Biochemistry 37*, 4592−4602.
57. Al-Shawi, M. K., Urbatsch, I. L., and Senior, A. E. (1994) Covalent inhibitors of P-glycoprotein ATPase activity, *J. Biol. Chem. 269*, 8986−8992.
58. Locher, K. P., Lee, A. T., and Rees, D. C. (2002) The *E. coli* BtuCD structure: a framework for ABC transporter architecture and mechanism, *Science 296*, 1091−1098.
59. Rosenberg, M. F., Callaghan, R., Modok, S., Higgins, C. F., and Ford, R. C. (2005) Three-dimensional structure of P-glycoprotein: the transmembrane regions adopt an asymmetric configuration in the nucleotide-bound state, *J. Biol. Chem. 280*, 2857−2862.
60. Rosenberg, M. F., Callaghan, R., Ford, R. C., and Higgins, C. F. (1997) Structure of the multidrug resistance P-glycoprotein to 2.5 nm resolution determined by electron microscopy and image analysis, *J. Biol. Chem. 272*, 10685−10694.
61. Hopfner, K. P., Karcher, A., Shin, D. S., Craig, L., Arthur, L. M., Carney, J. P., and Tainer, J. A. (2000) Structural biology of Rad50 ATPase: ATP-driven conformational control in DNA double-strand break repair and the ABC-ATPase superfamily, *Cell 101*, 789−800.
62. Polgar, O., Robey, R. W., Morisaki, K., Dean, M., Michejda, C., Sauna, Z. E., Ambudkar, S. V., Tarasova, N., and Bates, S. E. (2004) Mutational analysis of ABCG2: role of the GXXXG motif, *Biochemistry 43*, 9448−9456.
63. Loo, T. W., and Clarke, D. M. (1997) Identification of residues in the drug-binding site of human P-glycoprotein using a thiol-reactive substrate, *J. Biol. Chem. 272*, 31945−31948.
64. Loo, T. W., and Clarke, D. M. (1995) Membrane topology of a cysteine-less mutant of human P-glycoprotein, *J. Biol. Chem. 270*, 843−848.
65. Loo, T. W., and Clarke, D. M. (1999) Determining the structure and mechanism of the human multidrug resistance P-glycoprotein using cysteine-scanning mutagenesis and thiol-modification techniques, *Biochim. Biophys. Acta 1461*, 315−325.
66. Loo, T. W., and Clarke, D. M. (2000) The packing of the transmembrane segments of human multidrug resistance P-glycoprotein is revealed by disulfide cross-linking analysis, *J. Biol. Chem. 275*, 5253−5256.
67. Loo, T. W., and Clarke, D. M. (2000) Identification of residues within the drug-binding domain of the human multidrug resistance P-glycoprotein by cysteine-scanning mutagenesis and reaction with dibromobimane, *J. Biol. Chem. 275*, 39272−39278.
68. Loo, T. W., Bartlett, M. C., and Clarke, D. M. (2004) Disulfide cross-linking analysis shows that transmembrane segments 5 and 8 of human P-glycoprotein are close together on the cytoplasmic side of the membrane, *J. Biol. Chem. 279*, 7692−7697.
69. Stenham, D. R., Campbell, J. D., Sansom, M. S., Higgins, C. F., Kerr, I. D., and Linton, K. J. (2003) An atomic detail model for the human ATP binding cassette transporter P-glycoprotein derived from disulfide cross-linking and homology modeling, *FASEB J. 17*, 2287−2289.
70. Poelarends, G. J., and Konings, W. N. (2002) The transmembrane domains of the ABC multidrug transporter LmrA form a cytoplasmic exposed, aqueous chamber within the membrane, *J. Biol. Chem. 277*, 42891−42898.
71. Loo, T. W., and Clarke, D. M. (1996) The minimum functional unit of human P-glycoprotein appears to be a monomer, *J. Biol. Chem. 271*, 27488−27492.
72. Boscoboinik, D., Debanne, M. T., Stafford, A. R., Jung, C. Y., Gupta, R. S., and Epand, R. M. (1990) Dimerization of the P-glycoprotein in membranes, *Biochim. Biophys. Acta 1027*, 225−228.
73. Jette, L., Potier, M., and Beliveau, R. (1997) P-glycoprotein is a dimer in the kidney and brain capillary membranes: effect of cyclosporin A and SDZ-PSC 833, *Biochemistry 36*, 13929−13937.

74. Poruchynsky, M. S., and Ling, V. (1994) Detection of oligomeric and monomeric forms of P-glycoprotein in multidrug resistant cells, *Biochemistry 33*, 4163−4174 [erratum: (1994) *Biochemistry 33*, 9032].
75. Naito, M., and Tsuruo, T. (1992) Functionally active homodimer of P-glycoprotein in multidrug-resistant tumor cells, *Biochem. Biophys. Res. Commun. 185*, 284−290.
76. Juvvadi, S. R., Glavy, J. S., Horwitz, S. B., and Orr, G. A. (1997) Domain organization of murine mdr1b P-glycoprotein: the cytoplasmic linker region is a potential dimerization domain, *Biochem. Biophys. Res. Commun. 230*, 442−447.
77. Rosenberg, M. F., Mao, Q., Holzenburg, A., Ford, R. C., Deeley, R. G., and Cole, S. P. (2001) The structure of the multidrug resistance protein 1 (MRP1/ABCC1). Crystallization and single-particle analysis, *J. Biol. Chem. 276*, 16076−16082.
78. Soszynski, M., Kaluzna, A., Rychlik, B., Sokal, A., and Bartosz, G. (1998) Radiation inactivation suggests that human multidrug resistance-associated protein 1 occurs as a dimer in the human erythrocyte membrane, *Arch. Biochem. Biophys. 354*, 311−316.
79. Hori, S., Ohtsuki, S., Tachikawa, M., Kimura, N., Kondo, T., Watanabe, M., Nakashima, E., and Terasaki, T. (2004) Functional expression of rat ABCG2 on the luminal side of brain capillaries and its enhancement by astrocyte-derived soluble factor(s), *J. Neurochem. 90*, 526−536.
80. Eisenblatter, T., Huwel, S., and Galla, H. J. (2003) Characterisation of the brain multidrug resistance protein (BMDP/ABCG2/BCRP) expressed at the blood-brain barrier, *Brain Res. 971*, 221−231.
81. Bodo, A., Bakos, E., Szeri, F., Varadi, A., and Sarkadi, B. (2003) The role of multidrug transporters in drug availability, metabolism and toxicity, *Toxicol. Lett. 140−141*, 133−143.
82. Zhang, W., Mojsilovic-Petrovic, J., Andrade, M. F., Zhang, H., Ball, M., and Stanimirovic, D. B. (2003) The expression and functional characterization of ABCG2 in brain endothelial cells and vessels, *FASEB J. 17*, 2085−2087.
83. Ambudkar, S. V., Dey, S., Hrycyna, C. A., Ramachandra, M., Pastan, I., and Gottesman, M. M. (1999) Biochemical, cellular, and pharmacological aspects of the multidrug transporter, *Annu. Rev. Pharmacol. Toxicol. 39*, 361−398.
84. Andrus, M. B., Turner, T. M., Sauna, Z. E., and Ambudkar, S. V. (2000) The synthesis and evaluation of a solution phase indexed combinatorial library of non-natural polyenes for reversal of P-glycoprotein mediated multidrug resistance, *J. Org. Chem. 65*, 4973−4983.
85. Sauna, Z. E., Andrus, M. B., Turner, T. M., and Ambudkar, S. V. (2004) Biochemical basis of polyvalency as a strategy for enhancing the efficacy of P-glycoprotein (ABCB1) modulators: stipiamide homodimers separated with defined-length spacers reverse drug efflux with greater efficacy, *Biochemistry 43*, 2262−2271.

BI0503807